Versatile and Portable Cas12a-mediated Detection of Antibiotic Resistance Markers

Maryhory Vargas-Reyes[1,2], Roberto Alcántara[1,3,*], Soraya Alfonsi[3], Katherin Peñaranda[1,3], Dezemona Petrelli[3], Roberto Spurio[3], Monica J. Pajuelo[2], Pohl Milon[1,*]

[1]Biomolecules Laboratory, School of Biology, Faculty of Health Sciences, Universidad Peruana de Ciencias Aplicadas, Lima, Peru

[2]Laboratorio de Microbiología Molecular, Laboratorios de Investigación y Desarrollo, Facultad de Ciencias e Ingeniería, Universidad Peruana Cayetano Heredia, Lima, Peru

[3]School of Biosciences and Veterinary Medicine, University of Camerino, Camerino, Italy

[*]Correspondence: Pohl Milon: pmilon@upc.pe; Roberto Alcántara: roberto.alcantara@upc.pe

ABSTRACT

Antibiotic-resistant bacteria are spreading in clinical, industrial, and environmental ecosystems. The spreading dynamics to and from the environment are unknown, largely due to the lack of appropriate (robust, fast, low-cost) analytical assays. In this study, we developed C12a, a versatile molecular toolbox to detect genetic markers of antibiotic resistance using CRISPR/Cas12a. Biochemical characterization show that the C12a toolbox can detect less than 100 attoMolar of pure DNA fragments from the *blaCTX-M15* and *floR* genes, conferring resistance to b-lactams and amphenicols, respectively important for human and veterinary uses. In microbiological assays, C12a detected less than 10^2 CFU/mL and high concordance was observed if compared to antibiotic susceptibility tests, PCR, or to whole genome sequencing. Additionally, C12a confirmed a high prevalence of the integrase/integron system in *E. coli* isolates containing multiple antibiotic resistance genes (ARGs). The C12a toolbox shows equivalent detection performance in diverse laboratory settings, results redout (Fluorescence *vs* FLA) or input sample. Altogether, this work presents a comprehensive proof-of-concept, development description, and biochemical characterization of a collection of molecular tools to detect antibiotic resistance markers in a one health setup.

Keywords: Antibiotic Resistance Gene, Cas12a, *blaCTX*, *floR*, Integrase.

Introduction

The discovery of antibiotics allowed control of bacterial infections, improving surgical outcomes, treating infectious diseases, and boosting farm productivity, ultimately contributing to increased life expectancy [1]. However, the antimicrobial resistance (AMR) threat accelerated due to the combination of multiple interconnected factors, including antibiotic overuse[2], [3], complex ecological factors [4], [5], ineffective waste management and mechanisms of spread by horizontal gene transfer [6]. Effective surveillance strategies are lacking due to insufficient capacities for sensitive, timely, cost-effective, and accurate monitoring [7], [8]. Among the most concerning mechanisms are Extended Spectrum β-Lactamases (ESBLs) and resistance to amphenicols, due to their relevance for both human and animal health [9]. In Gram-negative bacteria, the *blaCTX-M-15* and *floR* are two of the most frequently reported antibiotic resistance genes (ARGs) within their respective classes, conferring resistance to β-lactam and amphenicol antibiotics, respectively (Figure 1A-B) [10]. While *blaCTX-M* [11], [12] variants have been primarily

associated with bacterial human isolates, *floR*[13], [14] has traditionally been linked to animal-derived bacterial isolates, as florfenicol is broadly used in livestock production. However, bacteria *floR*- positive strains are increasingly detected in humans, particularly among individuals in close contact to poultry [15]. Both ARGs have been detected in bacteria isolates from clinical[16], [17], [18], [19], community-acquired[12], [15], animal[13], [14], [20], [21], and environmental samples[10] including water[22], [23] and farms soil[23]. The ARGs spread is enhanced by mobile genetic elements (MGEs), due to their ability to move within and between different host species [24]. Among them, integrons are genetic elements that mobilize and express gene cassettes that confer resistance to antibiotics, disinfectants, heavy metal, and other pollutants [25]. Although integrons are not mobile on their own, they are frequently integrated within transposons or carried on plasmids, facilitating their horizontal transfer [26]. Class 1 integrons are the most prevalent in both clinical[27] and environmental [26], [28], [29] contexts, particularly in *Enterobacteriaceae* clinical strains, such as *E.coli* [30] (Figure 1C). Its relative abundance has been proposed as a marker of anthropogenic AMR pressure [31], since genomic analyses of cassette arrays frequently show co-occurrence with resistance to aminoglycoside, sulfonamide, tetracycline, β-lactams, and amphenicol [32], [33]. Due to its widespread distribution and frequent co-occurrence with multiple ARGs, detection of Class 1 integron could be used as a proxy to assess the ecological impact of human activity in AMR surveillance [25], [32].

Currently, different methods for detecting antimicrobial resistance (AMR) are used, with the most common being antimicrobial susceptibility testing (AST) and molecular techniques such as PCR, qPCR, and DNA sequencing [34], [35]. While these methods are considered standards, there is a need of assays with new technologies that combine the velocity provided by molecular methods with the low-costs of AST, and applicability in resource-limited or on-site settings. Target pre-amplification followed by nucleic acid detection using CRISPR technology has shown promising results due to the high specificity, sensitivity, low costs, and speed of the assay [36]. The molecular detection mechanism involves crRNA, a targeting sequence homologous to the gene of interest. crRNA hybridization with the complementary target region activates the Cas12a endonuclease, which then engages in trans-cleaving activity, cutting ssDNA non-specifically [37]. When using a fluorescence donor/quencher FRET pair placed into a ssDNA, this trans-cleaving activity generates an increase in fluorescence signal that can be detected using a wide range of laboratory set ups [38](Figure 1D).

Here, we present the C12a toolbox, a CRISPR-based set of molecular tools designed to detect genetic elements that confer antibiotic resistance or contribute to ARG propagation. The toolbox includes assays detecting *blaCTX-M-15* ($C12a^{bCTX}$), *floR* ($C12a^{FLO}$), and the *intI1* integrase gene ($C12a^{INT}$), selected for their relevance within the One Health framework. We describe the proof-of-concept, the biochemical and analytical characterization of C12a as an adaptable platform optimized for high-, and low-equipped laboratories in addition to an on-site portable setting (Figure 1C). Implementation of C12a nucleic acid-based technologies could effectively support fast, accurate, and sensitive detection, contributing to ARG surveillance efforts.

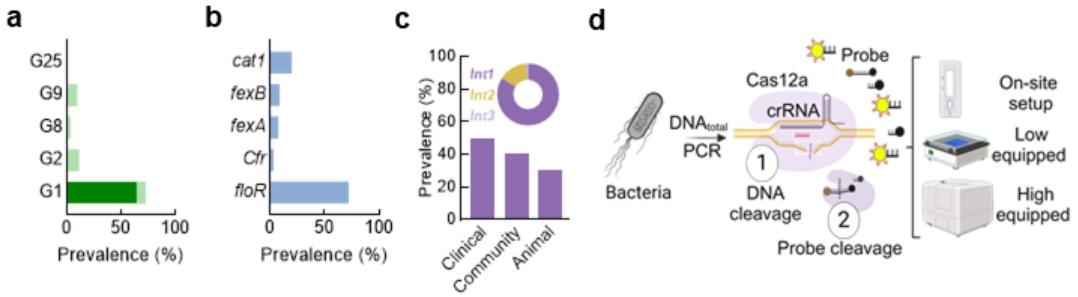

Figure 1. *blaCTX* and *floR* epidemiological context and the C12a rationale. (A) Prevalence and diversity of beta-lactamases in *E. coli* [11], [12]. The darker green bar represents the prevalence of the *blaCTX-M-15* gene within the Group 1. **(B)** Prevalence and diversity of amphenicol resistance genes in bacteria [13], [14]. **(C)** Prevalence of the Class 1 Integron across clinical [30], community, and animal settings [39]. The pie chart shows the three integron classes distribution in environmental isolates [40] **(D)** Scheme showing the C12a toolbox and the molecular mechanism of Cas12a-mediated detection, highlighting signal development, versatility, and portability.

Results

C12a Development

ARG detection sites were defined by comparing 61 *blaCTX-M-15* and 46 *floR* sequences from *E. coli* isolates available in GenBank [41] (Supplementary Dataset 1 and Dataset 2, respectively). Based on consensus sequences two primer sets for *blaCTX-M-15* and one for *floR* were selected to amplify regions containing a PAM sequence for Cas12a (TTTN) (Figure 2A, Figure S1, Table S2). Agarose gel electrophoresis confirmed amplification of *blaCTX-M-15* (216 bp) and *floR* (270 bp), with no bands in

103 negative controls (Figure S2). Amplicons were sequenced to confirm the presence of the expected target
104 DNA for each gene (Table S3). To optimize the crRNA/Cas12a reaction, two candidate crRNAs for each
105 target gene were designed to contain a complementary sequence to the amplified fragments (Table S2).
106 To determine sensitivity parameters, an initial test with increasing Mg^{2+} concentrations revealed an
107 optimal value of 20 mM, which was used in all assays. Both *blaCTX-M-15* and *floR* amplicons were
108 recognized by crRNA/Cas12a complex resulting in an increase in fluorescence signal (Figure S3) For
109 *blaCTX-M-15* target gene, primer set 2 combined with $crRNA^{CTX-2}$, showed greater fluorescence increase
110 compared to $crRNA^{CTX-1}$. For *floR* gene, $crRNA^{FLO-1}$ outperformed $crRNA^{FLO-2}$ (Figure S1). Thus,
111 $crRNA^{CTX-2}$ and $crRNA^{FLO-1}$ were selected for further assays. Regardless of template concentration,
112 $crRNA^{CTX}$ consistently generated a fluorescence signal faster than the *floR* crRNAs (Figure 2B and Figure
113 S1).

114 The results of this assay are reported as fluorescence ratio to the no-template control (NTC), indicated as
115 NF_{NTC} (a.u.). To calculate NF_{NTC}, each raw fluorescence value was divided by the corresponding value
116 from the NTC (Figure 2C). For the *blaCTX-M-15* gene, positive samples exhibited an NF_{NTC} of at least
117 14-fold, while negative samples display NF_{NTC} values near 1. Similarly, for the *floR* gene, positive
118 samples showed a 4-fold increase in NF_{NTC} compared to negative controls (Figure 2C and Figure S1).

119 Based on performance, the final detection systems were defined. For *blaCTX-M-15* detection, the
120 $C12a^{bCTX}$ system incorporates the primer set 2 and $crRNA^{CTX-2}$ (Table S2). On the other hand, $Cas12a^{FLO}$
121 detects *floR* using the primer set 1 and the $crRNA^{FLO-1}$ (Table S2).

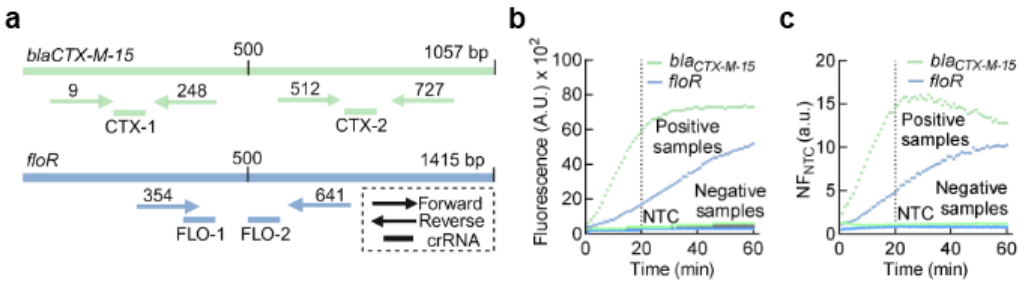

122

123 **Figure 2. Experimental setup for CRISPR/Cas12a-based assay development**. **(A)** Primers and crRNA
124 location on *blaCTX-M-15* and *floR* gene targets, ensuring coverage of PAM regions and complementary
125 crRNA areas. **(B)** Example of raw fluorescence readouts from CRISPR/Cas12a assays, showing a time-
126 dependent increase of the signal. Positive and negative controls, alongside the Non-Template Control
127 (NTC), are represented to illustrate the assay's ability to differentiate samples with or without ARGs. **(C)**

128 Example of normalized fluorescence ratio NF_{NTC} (a.u.) over time. In **(B)** and **(C),** the dotted line indicates
129 the 20-minute detection point, selected as the cut-off reading time for analysis.

130

131 **C12a Analytical Sensitivity**

132 Two key analytical parameters describe any given assay for analyte detection: the limit of blank (LoB;
133 also referred to as the cut-off) and the limit of detection (LoD). The average NF_{NTC} values for negative
134 samples using $C12a^{bCTX}$ or $C12a^{FLO}$ were 1.04 ± 0.02 and 0.94 ± 0.02 after 20 minutes of incubation
135 (Figure S4). Here we set the LoB as the average of true negative assays plus two standard deviations.
136 Thus, the resulting LoB values were 1.08 NF_{NTC} (a.u.) for $C12a^{bCTX}$ and 0.98 NF_{NTC} (a.u.) for $C12a^{FLO}$.
137 Based on these values, we can state that 95.45% of the values below the determined LoB were likely to be
138 classified as nonspecific background signals (i.e., signals in the absence of the analyte) (Figure S4).

139 To estimate the LoD for both detection systems, purified and quantified amplicons were tested at
140 increasing concentrations (from 10^{-18} to 10^{-8} M, atto to nanomolar). Averaged NF_{NTC} (a.u.) values,
141 measured at 10-minute intervals were used to define the lowest detectable target concentration at the
142 shortest reaction time. The LoD was calculated for each time interval, allowing the estimation of LoD as a
143 function of reaction time (Figure 3A). The time dependence indicates that after 21 minutes for $C12a^{bCTX}$
144 and 17 minutes for $C12a^{FLO}$, the LoD reached half of its maximum value, suggesting that a 20-minute
145 reaction time is a good compromise between assay speed and analytical sensitivity. The calculated LoD
146 for $C12a^{bCTX}$ and $C12a^{FLO}$ at 20 minutes was 70 aM and 50 aM, respectively (Figure 3B). Taking NF_{NTC}
147 values at times shorter than 20 minutes (i.e. 10 min) would result in a tenfold loss in sensitivity (Figure
148 3A).

149 We then assessed the analytical sensitivity of the CRISPR/Cas12a system in terms of the number of cells
150 carrying the resistance genes (Figure 3C). Bacterial cultures of true positive *E. coli* ranging from 3 to
151 $3x10^6$ CFU/mL were used (Figure S5). Non-linear fitting of the NF_{NTC} dependence on cell number (CFU)
152 allowed the calculation of the LoD. $C12a^{bCTX}$ reliably detected the *blaCTX-M-15* gene at 77 CFU/mL,
153 while $C12a^{FLO}$ required 173 CFU/mL to detect *floR* (Figure 3C). The lowest target concentration that
154 could be empirically detected for the two target genes, was 10 to 100 times lower compared to gel
155 electrophoresis analysis of PCR amplification (Figure 3D, E, and Figure S6). Altogether, the detection

156 and sensitivity performance of C12a^{bCTX} and C12a^{FLO} provide a solid foundation for testing the detection

157 systems on a larger number of samples (see below).

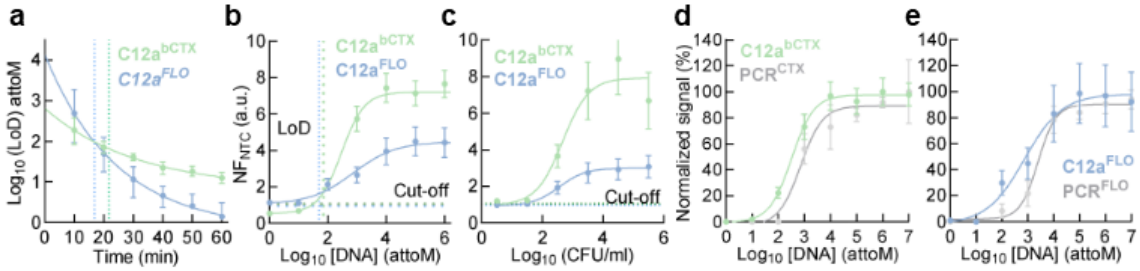

158

159 **Figure 3. C12a^{bCTX} and C12a^{FLO} Limit of Detection (LoD). (A)** Time-resolved determination of LoD
160 values for both ARGs Cas12a reactions, plotted on a logarithmic scale. The graph illustrates the LoD
161 decrease for C12a^{bCTX} and C12a^{FLO} over incubation time, with dotted lines marking the time-point when
162 the LoD reaches half of its maximum value. **(B)** Normalized fluorescence ratio as a function of target
163 concentration for ARG detection assays. The vertical dotted lines represent the LoD value calculated at 20
164 minutes, while the horizontal dotted lines represent NF$_{NTC}$ LoB (cutoff). **(C)** Normalized fluorescence
165 ratio over bacterial cell concentration for both C12a assays. The dotted horizontal lines indicate average
166 NF$_{NTC}$ cut-off values of 1.08 and 0.98 for C12a^{bCTX} and C12a^{FLO}, respectively. **(D)** Normalized assay
167 signals across target concentrations for C12a^{bCTX} detection compared to PCR-based detection evaluated
168 by gel electrophoresis. The fluorescent ratio for the Cas12a reaction and electrophoresis gel band
169 intensity, recorded as Area Under the Curve (AUC) values, are normalized as percentages to the highest
170 value. **(E)** Same as (D), but for C12a^{FLO}. Error bars in all panels represent standard deviations from 3
171 replicates.

172

173 **ARG detection in *E. coli* isolates by C12a^{bCTX} and C12a^{FLO}**

174 The presence of antibiotic resistance genes (ARGs) and the related phenotypic resistance in *E. coli*

175 isolates was assessed by two distinct assays: (i) molecular detection using the C12a toolbox and (ii)

176 antimicrobial susceptibility testing (AST) (Figure 4). Two small independent sample sets were randomly

177 selected from a collection of *E. coli* isolated from human sources in community settings (see Materials

178 and Methods). Fifteen isolates were evaluated for the presence of *blaCTX-M-15* and beta-lactam

179 resistance, while seventeen were assessed for *floR* and resistance to amphenicols. Phenotypic profiling

180 was confirmed using the combined disk (CD) method for ESBL detection and broth microdilution to

181 determine minimum inhibitory concentrations (MICs) for florfenicol (Table S4-5). The C12a^{bCTX} and

182 C12a^{FLO} assays were then applied to their corresponding set to evaluate detection performance.

183 Out of 15 isolates, 7 were ESBL producers and found positive by C12a^{bCTX} for the presence of *blaCTX-*
184 *M-15* gene while 8 were susceptible to beta lactams and found negative by the C12a toolbox (Figure 4A).
185 Similarly, C12a^{FLO} found the *floR* gene in 11 florfenicol resistant isolates, while susceptible isolates (6/17
186 isolates) turned out negatives by C12a (Figure 4C) (Table S4-5). When assessing the performance of the
187 C12a toolbox, NF_{NTC} values for ARG-positive samples ranged from 11 to 16 for C12a^{bCTX} and from 3 to
188 4.5 for C12a^{FLO} after 20 minutes of incubation, indicating the detection of the target genes. In contrast,
189 ARG-negative samples showed no NF_{NTC} values higher than 1.0 with both C12a assays, indicating the
190 absence of the target genes (Figure 4A-C). Altogether, the noise to signal ratio, for positive samples,
191 shown by the C12a toolbox was between 3- to 11- fold over the LoB. Full concordance was observed
192 between the presence of resistance genes using the C12a toolbox and AST assays (Figure 4B-D).

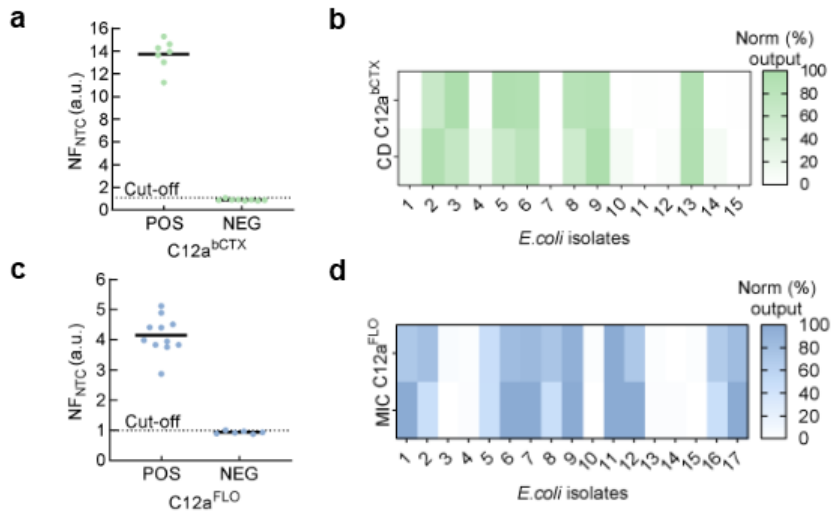

193

194 **Figure 4. C12a^{bCTX} and C12a^{FLO} comparison with AST methods. (a)** Distribution of *blaCTX-M-*15 in
195 17 isolates tested using the C12a^{bCTX} assay. The dotted line represents the LoB at 1.1. **(b)** Heat map
196 comparison of the C12a^{bCTX} assay with the disk diffusion test for AMR (CD). Results were normalized to
197 percentages, using the maximum value obtained for each dataset as 100%. **(c)** Similar to (a), but for the
198 C12a^{FLO} assay. The dotted line indicates the LoB at 1.0. **(d)** Similar to (b) but for the C12a^{FLO} assay with
199 microdilution test (MIC), showing that *floR* positive samples were phenotypically resistant to florfenicol.

200

201 **Detection of the *intI1* gene by C12a^{INT}**

202 Using the C12a toolbox, we evaluated the detection of the *intI1* integrase gene, located in the 5′ conserved
203 region of the Class 1 integron. Previous studies suggested a correlation between *intI1* presence and MDR

204 profiles [32], [33]. Here, we evaluated the detection of the *intI1* gene by designing a set of crRNAs
205 (C12a^{INT}) and using a reported set of primers [42] (Table S2) to detect a 146 bp amplification product
206 (Figure S7). Among the three candidate crRNAs, crRNA^{int1c} showed better NF_{NTC} values at 20 minutes
207 reaction time under standardized C12a reaction conditions (Figure 5A). Using the C12a^{INT}, we detected
208 the presence of the *intI1* gene in 17 out of 18 ARG-positive samples (Figure 5C). Fluorescence ratios over
209 the NTC control ranged between 3 to 10, showing greater dispersion if compared to the other C12a tools
210 (Figure 5B). Thus, the results could suggest that the presence of *intI1* is associated to *blaCTX-M-15* or
211 *floR*. However, several reports indicate that none of the evaluated ARG are usually located within the
212 gene cassette for integron 1. To get further insights, we investigated the correlation by *in silico* analysis of
213 sequencing data and characterize the integron structure and ARG content within cassette arrays (Figure
214 5C). Data analysis of short reads using *blaCTX-M15* or *floR* positive *E. coli* isolates revealed that 11/18
215 carried a cassette array (61.1 %), indicated by the presence of the attC recombination sites. The cassette
216 array frequently contained genes conferring resistance to aminoglycosides (100%), trimethoprim
217 (81.82%), phenicols (36.36%), lincosamide (27.27%) and sulfonamides (18.18%). Additionally, genes
218 conferring tolerance to disinfectants such as *qacE* were observed in 5 isolates (45.45%) (Figure 5C). The
219 *in-silico* analysis revealed that transposons localized near Class 1 Integron were probably involved in the
220 mechanism of acquisition and transfer of the observed cassette array. Consistent with previous reports,
221 *blaCTX-M-15* or *floR* genes were not found as part of the cassette arrays (Table S7). Our results suggest
222 the potential of C12a^{INT} for Class 1 integron detection as proxy of multidrug resistance as previously
223 described [32], [33], however, direct ARG detection remains necessary for surveillance of specific genetic
224 markers of antibiotic resistance.
225

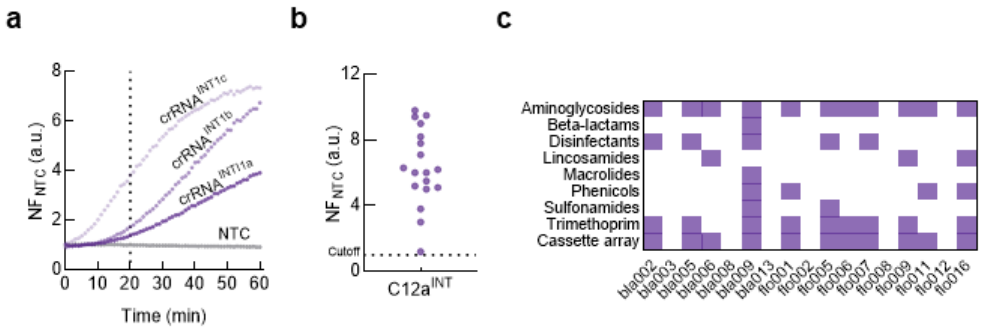

226

227 **Figure 5. C12a^{INT} detects the *intI1* gene, as potential indicator of multidrug resistant *E. coli.* (A)**
228 Time-course of normalized fluorescence development for the C12a^{INT} assay with three crRNA designed to
229 detect the *intI1* gene. The vertical dotted line represents the incubation time used. **(B)** CRISPR-Cas

230 detection of *intI1* gene in 18 ARG-positive isolates tested using the C12a^{INT} assay. The dotted line
231 represents the LoB at 1.0. **(C)** Heat map summarizing the antibiotic resistance genes related to different
232 antibiotic families identified within the Class 1 integron cassette array of the ARG-positive *E. coli*
233 isolates used in this study. ARGs were identified by bioinformatic analysis of genome sequencing data
234 (BioProject number PRJNA821865).

235

236 **Efficient C12a-mediated ARGs detection in different laboratory setups**

237 Differences in equipment availability may impact on the analytical performance of the C12a detection
238 toolbox. To address this, we adapted our detection assays to three laboratory setups: i) Low-equipped
239 with minimal tools for qualitative readouts, such as a thermocycler and a transilluminator; ii) portable
240 setup using the Lateral Flow Assay (LFA) and transportable workstation (BentoLab®) suitable for on-site
241 analysis, and iii) High equipped with a multimode microplate reader for quantitative analysis, as used
242 here for assay validation (Figure 6).

243 Fourteen purified total fecal DNA available from the stool sample repository (BioProject number
244 PRJNA821865) were analyzed with the C12a^{bCTX} and C12a^{FLO} assays across the three laboratory set-ups.
245 For low equipped setup, direct visualization using a blue light transilluminator showed fluorescence in
246 five out of 7 samples for *blaCTX-M-15*. For *floR*, six out of seven samples resulted in fluorescence
247 observation (Figure 6A). The high-equipped setup showed that C12a^{bCTX} detected *blaCTX-M-15* in five
248 samples, and two samples tested negative, respectively. All positive samples showed NF_{NTC} (a.u.) values
249 exceeding 6 within 20 minutes. Similarly, for the C12a^{FLO}, NF_{NTC} (a.u.) values surpassing 3 were
250 recorded at 20 minutes (Figure 6B). For on-site setups, detection relied on LFA readouts instead of
251 fluorescence detection. Here, a double-labeled probe with FITC and biotin is added in the CRISPR-Cas
252 system allowing the appearance of two bands (the control line and test line) on the strip when an ARG is
253 detected (Figure 6C). No difference in detection performance was observed across all setups evaluated.
254 Although the sample size was limited, these results suggest that the C12a toolbox demonstrates sufficient
255 analytical sensitivity and robustness for ARG detection in total DNA samples across different laboratory
256 setups.

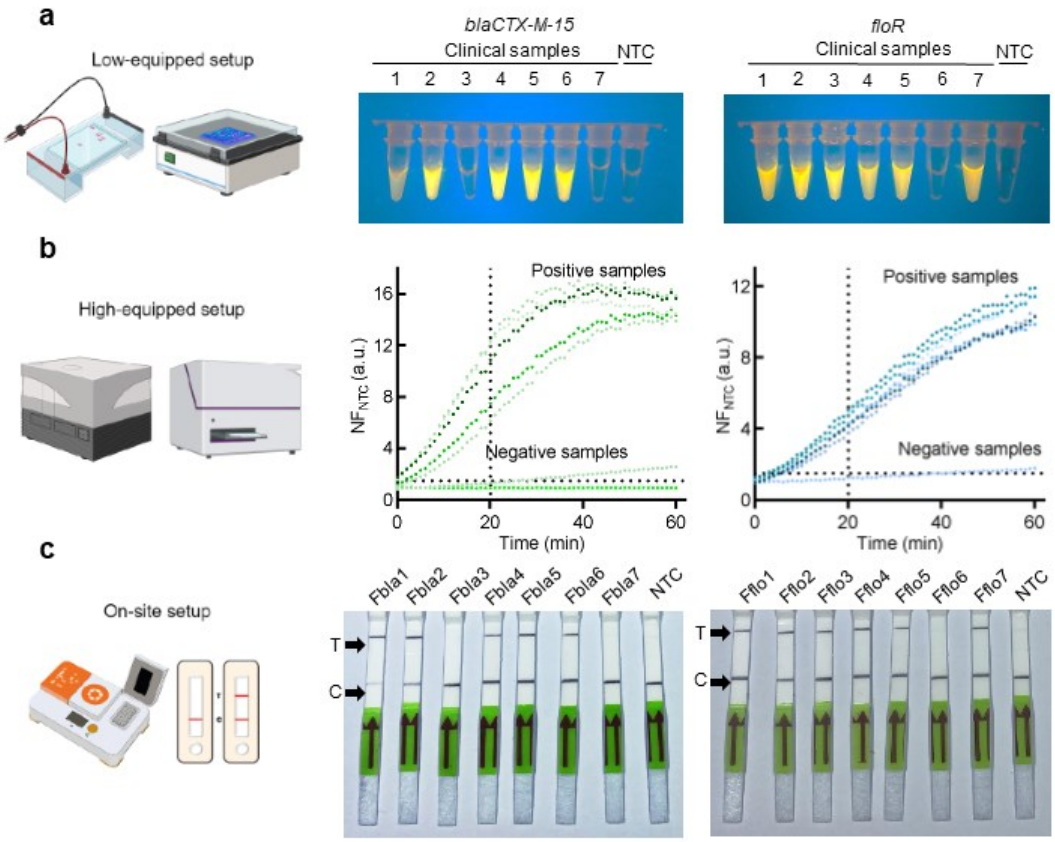

Figure 6. C12a application across different laboratory setups. (A) *blaCTX-M-15* and *floR* detection in a low-equipped laboratory setup. Fluorescence was observed by direct visualization and photographed with a smartphone camera, default settings using a blue light transilluminator. **(B)** Similar to (A), but for a high-equipped laboratory. NF_{NTC} (a.u.) values were measured over 60 minutes with a 20-minute detection cutoff. The horizontal dotted line represents an average NF_{NTC} cut-off value of 1.0. **(C)** Similar to (A), but for an on-site setup. Detection by LFA strips readouts at 15 minutes incubation, where the T bands indicate the positivity of the test and C bands correspond to the control. NTC refers to non-template control.

Discussion

The global challenge of antimicrobial resistance (AMR) needs the development of new molecular detection strategies that are rapid, sensitive, cost-effective, and adaptable to diverse contexts, including clinical, veterinary, and environmental settings. While established platforms such as antimicrobial susceptibility testing (AST), PCR, and whole-genome sequencing (WGS) are solid approaches, they remain limited by infrastructure requirements, cost, or turnaround time [34], [35]. In this study, we

273 presented the proof-of-concept of C12a for detecting key antibiotic resistance genes (ARGs) and
274 associated elements. Although not yet validated for clinical or diagnostic use, the C12a toolbox
275 demonstrates promising analytical features that could support future diagnostic development and
276 surveillance efforts.

277 Molecular detection by C12a display distinctive features: rapid (20 min detection, 100 minutes total
278 analysis), competitive low limits of detection, and support for multiple readout formats, that make it
279 suitable for various applications. CRISPR-Cas-based assays have demonstrated analytical performance
280 comparable to well established techniques, including qPCR, which remains the reference method in most
281 molecular detection workflows [43]. Previous studies showed complete concordance between CRISPR-
282 Cas and qPCR results for the detection of genetic elements in pathogenic and virulence targets [44], [45],
283 [46], [47], [48]. The high specificity of C12a systems aligns with other CRISPR-Cas assays thanks to the
284 dual recognition steps mechanism, which involves both primer selection and crRNA binding. While a
285 direct comparison with qPCR was not conducted in this study, the C12a system showed strong signal-to-
286 noise ratios, well-defined limits of blank (LoB), low limits of detection (LoD), and full concordance with
287 both AST and WGS analysis, reinforcing the reliability of the detection setup. Additionally, the LoD
288 obtained for the C12a toolbox is consistent with those reported in other CRISPR-based studies [43], [49].

289 The targets selected for this study address both diagnostic relevance and ecological concern. Detection of
290 *blaCTX-M-15* and *floR* genes are of increasing importance due to their widespread distribution across
291 human, animal and environmental interfaces[10] (Figure 1A). Specifically, *blaCTX-M-15*[20], [21] has
292 been traditionally associated with humans and *floR*[15], [18], [19] with animals, however recent findings
293 indicate that both genes are now being detected across diverse scenarios. Resistance gene *floR*, mainly
294 linked to animal populations, has been recently identified in humans, highlighting its spread beyond
295 conventional boundaries [15]. These patterns of occurrence reflect the interconnected dynamics of AMR,
296 where elements like Class 1 integrons, often inserted in transposons and plasmids, contribute to the spread
297 of multidrug-resistant genes in various environments[33]. Although our analysis revealed no integron
298 association for *blaCTX-M-15* or *floR* in the tested isolates, the frequent co-occurrence of *intI1* with other
299 ARGs highlights its utility as a marker of anthropogenic AMR pressure[25], [28], [32], [33].

300 A key feature of the C12a toolbox is its adaptability to laboratories with varying levels of infrastructure.
301 C12a was successfully used with high-end equipment settings using fluorescence microplate readers, in

302 low-tech settings using basic fluorescence visualization, and in portable formats using lateral flow assays
303 (LFA). Performance was consistent across platforms, with only modest reductions in sensitivity observed
304 in low-resource setups. These results suggest that the C12a system could support surveillance workflows
305 in resource-limited environments, although further testing and optimization for varying sample types
306 (e.g., water, soil) and including other bacterial species are needed. Furthermore, while the system offers a
307 strong biochemical and analytical foundation, clinical diagnostic application will require rigorous
308 validation as by regulatory guidelines. Integration with mobile data platforms may also enhance usability
309 for surveillance or epidemiological purposes.
310 In summary, this work presents a validated proof-of-concept for a CRISPR-Cas12a-based molecular
311 detection system targeting AMR gene markers. Although not yet suitable for diagnostic implementation,
312 the C12a toolbox demonstrates key features (velocity, sensitivity, specificity, and versatility) that are
313 essential for future development of low-cost, field-adaptable AMR surveillance tools within a One Health
314 framework.

315

316 Materials and Methods

317 Biological samples

318 Two types of biological samples were used to evaluate the performance and adaptability of the C12a
319 toolbox: (i) Total DNA extracted from *Escherichia coli* isolates obtained from fecal samples and (ii) total
320 DNA extracted directly from fecal material. All samples originated from a previously conducted
321 community-based study involving children in Lima, Peru (NIH R01AI108695-01A1) [50], which
322 received ethical approval from the institutional review board at Universidad Peruana Cayetano Heredia
323 (UPCH). No demographic or identifying metadata from participants were accessed for this study. A
324 subset of positive and negative isolates for *blaCTX-M-15* (bla001 – bla015, Table S4) and *flor* (flo001 –
325 flo0017, Table S5) was randomly selected for the study. Only *E. coli* isolates positive for *blaCTX-M-15*
326 or *floR* were tested for the Class 1 integron detection. Total fecal DNA from a subset of samples (Fbla1 –
327 Fbla7, and Fflo1 – Fflo7; Table S6) was used to evaluate the adaptability of the CRISPR assays across
328 three laboratory configurations, including high-, low-, and portable-equipment settings.

329 Molecular stocks

330 *DNA purification:* Total DNA was extracted from an *E. coli* culture grown to OD_{600} = 0.7 using the Quick
331 DNA Miniprep kit (Cat # D4069, Zymo Research) following the manufacturer's protocol. DNA was
332 quantified using a NanoDrop spectrophotometer and stored at -20°C. Amplicons were purified using the
333 Oligo Clean Kit (Cat # D4060, Zymo Research). *Oligonucleotides synthesis:* Primers and crRNA DNA
334 sequences were sourced from Macrogen Inc. (Seoul, South Korea). *crRNA synthesis:* crRNA was
335 synthesized by *in vitro* transcription using the TranscriptAid T7 High Yield Transcription Kit
336 (Cat#K0411, ThermoFisher Scientific) and purified with the RNA Clean & Concentrator Kit (Cat #11-
337 353B, Zymo Research). *Enzymes:* Taq DNA polymerase and Cas12a proteins were sourced from locally
338 expressed and purified stocks stored at -80°C, as detailed in [51].

339 **Antimicrobial susceptibility test**

340 *Combined disk test*: The antibiotic susceptibility profile of 32 *E. coli* isolates was determined by the disk
341 diffusion method, using *E. coli* ATCC 25922 (Cat # 0335, Lab Elite) as the control strain. *E. coli* isolates
342 from glycerol stocks were streaked on LB agar plates and incubated overnight at 37°C. Isolated colonies
343 were resuspended in 0.9% saline solution to a density of 0.5 McFarland and swabbed onto Mueller-
344 Hinton agar plates (Cat # M173-500G, Himedia). Antibiotic disks, including cefotaxime (CTX) 30 µg
345 (Cat # 9017, Liofilchem), and ceftazidime (CAZ) 30 µg (Cat # 9019, Liofilchem) were placed on the
346 surface of the medium. After 18 hours of incubation at 37°, inhibition zones were measured and
347 interpreted following the CLSI guidelines. A confirmatory test for ESBL production, recommended by
348 CLSI[52], was performed using CTX 30 µg and CAZ 30 µg disks combined with clavulanic acid:
349 CTX/AC 40 µg (Cat # 9182, Liofilchem), and CAZ/AC 40 µg (Cat # 9145, Liofilchem). Plates were
350 incubated for 18 hours at 37°C, and ESBL producers were detected by measuring the difference in the
351 inhibition halo of the antibiotic in the presence of clavulanic acid (>5 mm). *Broth microdilution assay*:
352 Florfenicol (Cat #F1427-500MG, Merck) was dissolved in dimethyl sulfoxide (DMSO) to a concentration
353 of 100 mg/ml. Serial dilutions, ranging from 256 µg/ml to 0.125 µg/ml were prepared in a 96-well plate
354 (Cat # 3596, ThermoFisher) using Mueller- Hinton Broth II (Cat # 610218, Liofilchem). Each well was
355 inoculated with 1.5 x 10^6 CFU/ml of cells. After 18 h of incubation at 37°C, the MIC was determined
356 according to CLSI guidelines[53]. A MIC value of 32 µg/mL has been proposed as a tentative threshold
357 to identify florfenicol-resistant *E. coli* isolates harboring the *floR* gene [54]. However, it does not
358 represent a formally established clinical breakpoint.

359 **Bioinformatic analysis**

360 To identify detection targets, all available *E. coli* resistance gene sequences for *blaCTX-M-15* and *floR* in
361 GenBank as of January 2022 were collected. Multiple alignment was performed, obtaining a consensus
362 sequence of 1057 bp for *blaCTX-M-15* and 1415 bp for *floR* (Supplementary Dataset 1 and Dataset
363 2, respectively). Primer sets were designed for the *blaCTX-M-15* [16] and *floR* [19]genes. For crRNA
364 guide design and evaluation, CRISPRscan and Chop-Chop bioinformatics tools were used [55], [56].
365 DNA data analysis was downloaded from the BioProject web portal of the NCBI
366 (https://www.ncbi.nlm.nih.gov/bioproject/) using accession code PRJNA821865. ARG presence was
367 evaluated using the ResFinder platform (http://genepi.food.dtu.dk/resfinder) v4.6.0 [57] with default
368 parameters. Briefly, a minimum length of 60% and a threshold of 90% were set up for ARG and
369 disinfectant-resistance gene identification. *E.coli* was defined as the species input. For the identification
370 of the integrase-integron class 1, the VRprofile2 platform (https://tool2-mml.sjtu.edu.cn/VRprofile/)[58]
371 with default parameters. Fluorescence data from the Synergy H1 plate reader were collected using Gen 5
372 software and exported to Excel. NF_{ntc} values were calculated during data processing and analysis as
373 appropriate. All fluorescence data analysis and chart preparation were performed using GraphPad Prism
374 version 10.0.0, www.graphpad.com.

375 **C12a Molecular Assays**

376 *DNA amplification and analysis:* PCR conditions for amplifying the *blaCTX-M-15* and *floR* targets
377 included an initial denaturation at 95°C for 3 minutes, followed by 30 cycles of denaturation at 95° for 30
378 sec, annealing at 59°C for 30 sec, extension at 72°C for 30 sec, and a final extension at 72°C for 5
379 minutes. For the *intI1* gene target, an annealing temperature of 60°C was used. Amplification reactions
380 (20 µL) contained 2 ng/µL Taq DNA polymerase, 0.2 µM primers, and 1 to 10 ng/µl of DNA in RPB1X
381 buffer (Table S1). PCR products were visualized using 1.7% agarose gel electrophoresis (Cat # CSL-
382 AG500, Cleaver Scientific) in 1X TBE buffer (Table S1) at 80 V for 1 hour. Gels were stained with 6X
383 Trick-Track – SYBR Gold (Cat #R1161, ThermoFisher) and visualized with a Gel Doc system (Bio-Rad)
384 using the Sybergold option. A 100 bp molecular weight marker (Cat #SM0242, Thermo Scientific) was
385 included. Band intensity was quantified as AUC using Gel Analyzer v23 (www.gelanalyzer.com).

386 *crRNA/Cas12a-mediated detection:* 150 nM crRNA was refolded (65°C for 10 minutes, followed by 10
387 minutes at 25°C) and assembled with 100 nM Cas12a, and 2 µM FAM probe (6-FAM/TTATT/3IABkFQ)

388 in CRB1 buffer (Table S1) in the dark for 10 minutes. Unpurified PCR reactions containing amplicons (5
389 µL) were combined with 10 µL of the complex in CRB2 buffer (Table S1) to a final volume of 100 µL.
390 Fluorescence was measured using a plate reader (Synergy H1, BioTek Instruments) with excitation at 491
391 nm and emission at 525 nm.

392 *Lateral Flow Assay (LFA):* CRISPR-Cas reaction was performed as described above using a
393 biotin/fluorescein probe (6-FAM/TTATTATT/BIOTIN). The reaction buffer was supplemented with
394 polyethylene glycol (Cat # 25322-68-3, Merck) to a final concentration of 5%. After 30 minutes of
395 incubation, a LFA strip (Cat # 3822-9000, Milenia Biotec GmbH) was submerged in the reaction. The
396 signal on the strips was detected after 5-10 minutes.

397 *LoB and LoD determination*: Pure genomic DNA from ten susceptible *E. coli* isolates (true negative)
398 were used to determine the LoB, using the formula LoB = Avg_NF_{NTC} + 2 SD (where "Avg" is average
399 NF_{ntc} values, and "SD" is standard deviation). The LoD was determined using both amplification products
400 and bacterial cell counts for the *blaCTX-M-15* and *floR* targets. Amplicons were purified using the Oligo
401 Clean Kit (Cat # D4060, Zymo Research) and quantified by absorbance at 260nm. DNA concentrations
402 ranged from 1 aM to 10 nM. The LoD was then estimated as the lowest DNA concentration above the
403 LoB + 2SD [59]. For the bacterial cell LoD determination, a curve was generated using a positive *E. coli*
404 isolate culture. Starting from a cell density of 0.5 McFarland, and 7 ten-fold dilutions in duplicate. One
405 set of dilutions was plated on LB agar plates for CFU counting, while the other set was analyzed directly
406 with C12a.

407 References

408

409 [1] Hutchings, M. I., Truman, A. W. & Wilkinson, B. Antibiotics: past, present and
410 future. *Curr Opin Microbiol* **51**, 72–80 (2019).

411 [2] Lipsitch, M. & Samore, M. H. Antimicrobial Use and Antimicrobial Resistance: A
412 Population Perspective. *Emerg Infect Dis* **8**, 347–354 (2002).

413 [3] Bungau, S., Tit, D. M., Behl, T., Aleya, L. & Zaha, D. C. Aspects of excessive
414 antibiotic consumption and environmental influences correlated with the occurrence of
415 resistance to antimicrobial agents. *Curr Opin Environ Sci Health* **19**, 100224 (2021).

416 [4] Huijbers, P. M. C. *et al.* Role of the Environment in the Transmission of
417 Antimicrobial Resistance to Humans: A Review. *Environ Sci Technol* **49**, 11993–12004
418 (2015).

419 [5] Zhang, Z. *et al.* Assessment of global health risk of antibiotic resistance genes. *Nat*
420 *Commun* **13**, 1553 (2022).

421 [6] von Wintersdorff, C. J. H. *et al.* Dissemination of Antimicrobial Resistance in
422 Microbial Ecosystems through Horizontal Gene Transfer. *Front Microbiol* **7**, (2016).

423 [7] Arnold, K. E. *et al.* The need for One Health systems-thinking approaches to
424 understand multiscale dissemination of antimicrobial resistance. *Lancet Planet Health*
425 **8**, e124–e133 (2024).

426 [8] Samreen, Ahmad, I., Malak, H. A. & Abulreesh, H. H. Environmental antimicrobial
427 resistance and its drivers: a potential threat to public health. *J Glob Antimicrob Resist*
428 **27**, 101–111 (2021).

429 [9] Aslam, B. *et al.* Antibiotic Resistance: One Health One World Outlook. *Front Cell*
430 *Infect Microbiol* **11**, (2021).

431 [10] Zhuang, M. *et al.* Distribution of antibiotic resistance genes in the environment.
432 *Environmental Pollution* **285**, 117402 (2021).

433 [11] Mazumder, R., Abdullah, A., Ahmed, D. & Hussain, A. High Prevalence of
434 blaCTX-M-15 Gene among Extended-Spectrum β-Lactamase-Producing Escherichia
435 coli Isolates Causing Extraintestinal Infections in Bangladesh. *Antibiotics* **9**, 796 (2020).

436 [12] Akenten, C. W. *et al.* Carriage of ESBL-producing Klebsiella pneumoniae and
437 Escherichia coli among children in rural Ghana: a cross-sectional study. *Antimicrob*
438 *Resist Infect Control* **12**, 60 (2023).

439 [13] Li, P. *et al.* Analysis of Resistance to Florfenicol and the Related Mechanism of
440 Dissemination in Different Animal-Derived Bacteria. *Front Cell Infect Microbiol* **10**,
441 (2020).

442 [14] Ying, Y. *et al.* Florfenicol Resistance in Enterobacteriaceae and Whole-Genome
443 Sequence Analysis of Florfenicol-Resistant *Leclercia adecarboxylata* Strain R25. *Int J*
444 *Genomics* **2019**, 1–10 (2019).

445 [15] Murray, M. *et al.* Market Chickens as a Source of Antibiotic-Resistant Escherichia
446 coli in a Peri-Urban Community in Lima, Peru. *Front Microbiol* **12**, (2021).

447 [16] Ramadan, A. A., Abdelaziz, N. A., Amin, M. A. & Aziz, R. K. Novel blaCTX-M
448 variants and genotype-phenotype correlations among clinical isolates of extended
449 spectrum beta lactamase-producing Escherichia coli. *Sci Rep* **9**, 4224 (2019).

450 [17] Negeri, A. A. *et al.* Characterization of plasmids carrying blaCTX-M genes among
451 extra-intestinal Escherichia coli clinical isolates in Ethiopia. *Sci Rep* **13**, 8595 (2023).

452 [18] Lu, J. *et al.* Spread of the florfenicol resistance floR gene among clinical Klebsiella
453 pneumoniae isolates in China. *Antimicrob Resist Infect Control* **7**, 127 (2018).

454 [19] Qian, C. *et al.* Identification of floR Variants Associated With a Novel Tn4371-
455 Like Integrative and Conjugative Element in Clinical Pseudomonas aeruginosa Isolates.
456 *Front Cell Infect Microbiol* **11**, (2021).

457 [20] Gundran, R. S. *et al.* Prevalence and distribution of blaCTX-M, blaSHV, blaTEM
458 genes in extended- spectrum β- lactamase- producing E. coli isolates from broiler farms
459 in the Philippines. *BMC Vet Res* **15**, 227 (2019).

460 [21] Higgins, O. *et al.* Portable Differential Detection of CTX-M ESBL Gene Variants,
461 $bla_{\text{CTX-M-1}}$ and $bla_{\text{CTX-M-15}}$, from Escherichia coli Isolates and Animal Fecal Samples
462 Using Loop-Primer Endonuclease Cleavage Loop-Mediated Isothermal Amplification.
463 *Microbiol Spectr* **11**, (2023).

464 [22] Rangama, S. *et al.* Mechanisms Involved in the Active Secretion of CTX-M-15 β-
465 Lactamase by Pathogenic Escherichia coli ST131. *Antimicrob Agents Chemother* **65**,
466 (2021).

467 [23] Liao, C.-Y. *et al.* Antimicrobial Resistance of Escherichia coli From Aquaculture
468 Farms and Their Environment in Zhanjiang, China. *Front Vet Sci* **8**, (2021).

469 [24] Tokuda, M. & Shintani, M. Microbial evolution through horizontal gene transfer by
470 mobile genetic elements. *Microb Biotechnol* **17**, (2024).

471 [25] Gillings, M. R. *et al.* Using the class 1 integron-integrase gene as a proxy for
472 anthropogenic pollution. *ISME J* **9**, 1269–1279 (2015).

473 [26] Zhang, S. *et al.* Dissemination of antibiotic resistance genes (ARGs) via integrons
474 in Escherichia coli: A risk to human health. *Environmental Pollution* **266**, 115260
475 (2020).

476 [27] Bhat, B. A. *et al.* Integrons in the development of antimicrobial resistance: critical
477 review and perspectives. *Front Microbiol* **14**, (2023).

478 [28] Corno, G. *et al.* Class 1 integron and related antimicrobial resistance gene
479 dynamics along a complex freshwater system affected by different anthropogenic
480 pressures. *Environmental Pollution* **316**, 120601 (2023).

481 [29] Stalder, T., Barraud, O., Casellas, M., Dagot, C. & Ploy, M.-C. Integron
482 Involvement in Environmental Spread of Antibiotic Resistance. *Front Microbiol* **3**,
483 (2012).

484 [30] Halaji, M. *et al.* The Global Prevalence of Class 1 Integron and Associated
485 Antibiotic Resistance in *Escherichia coli* from Patients with Urinary Tract Infections, a
486 Systematic Review and Meta-Analysis. *Microbial Drug Resistance* **26**, 1208–1218
487 (2020).

488 [31] Stedtfeld, R. D. *et al.* Isothermal assay targeting class 1 integrase gene for
489 environmental surveillance of antibiotic resistance markers. *J Environ Manage* **198**,
490 213–220 (2017).

491 [32] Rao, S., Maddox, C. W., Hoien-Dalen, P., Lanka, S. & Weigel, R. M. Diagnostic
492 Accuracy of Class 1 Integron PCR Method in Detection of Antibiotic Resistance in
493 *Salmonella* Isolates from Swine Production Systems. *J Clin Microbiol* **46**, 916–920
494 (2008).

495 [33] Solis, M. N. *et al.* Detecting Class 1 Integrons and Their Variable Regions in
496 Escherichia coli Whole-Genome Sequences Reported from Andean Community
497 Countries. *Antibiotics* **13**, 394 (2024).

498 [34] Abramova, A., Berendonk, T. U. & Bengtsson-Palme, J. A global baseline for
499 qPCR-determined antimicrobial resistance gene prevalence across environments.
500 *Environ Int* **178**, 108084 (2023).

501 [35] Abramova, A., Karkman, A. & Bengtsson-Palme, J. Metagenomic assemblies tend
502 to break around antibiotic resistance genes. *BMC Genomics* **25**, 959 (2024).

503 [36] Li, S.-Y. *et al.* CRISPR-Cas12a-assisted nucleic acid detection. *Cell Discov* **4**, 20
504 (2018).

505 [37] Chen, J. S. *et al.* CRISPR-Cas12a target binding unleashes indiscriminate single-
506 stranded DNase activity. *Science (1979)* **360**, 436–439 (2018).

507 [38] Broughton, J. P. *et al.* CRISPR–Cas12-based detection of SARS-CoV-2. *Nat*
508 *Biotechnol* **38**, 870–874 (2020).

509 [39] Karimi Dehkordi, M., Halaji, M. & Nouri, S. Prevalence of class 1 integron in
510 Escherichia coli isolated from animal sources in Iran: a systematic review and meta-
511 analysis. *Trop Med Health* **48**, 16 (2020).

512 [40] Fadare, F. T., Fadare, T. O. & Okoh, A. I. Prevalence, molecular characterization
513 of integrons and its associated gene cassettes in Klebsiella pneumoniae and K. oxytoca
514 recovered from diverse environmental matrices. *Sci Rep* **13**, 14373 (2023).

515 [41] Nadimpalli, M. L. *et al.* Effects of breastfeeding on children's gut colonization
516 with multidrug-resistant Enterobacterales in peri-urban Lima, Peru. *Gut Microbes* **16**,
517 (2024).

518 [42] Zhang, Y., Lu, J., Wu, J., Wang, J. & Luo, Y. Potential risks of microplastics
519 combined with superbugs: Enrichment of antibiotic resistant bacteria on the surface of
520 microplastics in mariculture system. *Ecotoxicol Environ Saf* **187**, 109852 (2020).

521 [43] Kaminski, M. M., Abudayyeh, O. O., Gootenberg, J. S., Zhang, F. & Collins, J. J.
522 CRISPR-based diagnostics. *Nat Biomed Eng* **5**, 643–656 (2021).

523 [44] Wang, B. *et al.* Cas12aVDet: A CRISPR/Cas12a-Based Platform for Rapid and
524 Visual Nucleic Acid Detection. *Anal Chem* **91**, 12156–12161 (2019).

525 [45] Curti, L. A. *et al.* CRISPR-based platform for carbapenemases and emerging
526 viruses detection using Cas12a (Cpf1) effector nuclease. *Emerg Microbes Infect* **9**,
527 1140–1148 (2020).

528 [46] Wang, X. *et al.* Development and clinical application of a novel CRISPR-Cas12a
529 based assay for the detection of African swine fever virus. *BMC Microbiol* **20**, 282
530 (2020).

531 [47] Wang, D. *et al.* A CRISPR/Cas12a-based DNAzyme visualization system for
532 rapid, non-electrically dependent detection of *Bacillus anthracis*. *Emerg Microbes*
533 *Infect* **11**, 429–438 (2022).

534 [48] van Dongen, J. E. & Segerink, L. I. Building the Future of Clinical Diagnostics: An
535 Analysis of Potential Benefits and Current Barriers in CRISPR/Cas Diagnostics. *ACS*
536 *Synth Biol* **14**, 323–331 (2025).

537 [49] Zhou, J., Li, Z., Seun Olajide, J. & Wang, G. CRISPR/Cas-based nucleic acid
538 detection strategies: Trends and challenges. *Heliyon* **10**, e26179 (2024).

539 [50] Pajuelo, M. J. *et al.* Epidemiology of enterotoxigenic Escherichia coli and impact
540 on the growth of children in the first two years of life in Lima, Peru. *Front Public*
541 *Health* **12**, (2024).

542 [51] Mendoza-Rojas, G. *et al.* A low-cost and open-source protocol to produce key
543 enzymes for molecular detection assays. *STAR Protoc* **2**, 100899 (2021).

544 [52] CLSI. *Performance Standards for Antimicrobial Susceptibility Testing; Twenty-*
545 *First Informational Supplement M100-S21*. (Wayne, PA, 2020).

546 [53] CLSI. *Methods for Dilution Antimicrobial Susceptibility Tests for Bacteria That*
547 *Grow Aerobically M07-Ed12*. (Wayne, PA, 2024).

548 [54] Singer, R. S. *et al.* Relationship between Phenotypic and Genotypic Florfenicol
549 Resistance in *Escherichia coli*. *Antimicrob Agents Chemother* **48**, 4047–4049 (2004).

550 [55] Labun, K. *et al.* CHOPCHOP v3: expanding the CRISPR web toolbox beyond
551 genome editing. *Nucleic Acids Res* **47**, W171–W174 (2019).

552 [56] Moreno-Mateos, M. A. *et al.* CRISPRscan: designing highly efficient sgRNAs for
553 CRISPR-Cas9 targeting in vivo. *Nat Methods* **12**, 982–988 (2015).

554 [57] Bortolaia, V. *et al.* ResFinder 4.0 for predictions of phenotypes from genotypes.
555 *Journal of Antimicrobial Chemotherapy* **75**, 3491–3500 (2020).

556 [58] Wang, M. *et al.* VRprofile2: detection of antibiotic resistance-associated mobilome
557 in bacterial pathogens. *Nucleic Acids Res* **50**, W768–W773 (2022).

558 [59] CLSI. *Evaluation of Detection Capability for Clinical Laboratory Measurement*
559 *Procedures; Approved Guideline. CLSI Document EP17-A2.* (Clinical and Laboratory
560 Standards Institute, Wayne, PA, 2012).

561

562 ## Ethics

563 The *E. coli* isolates and DNA fecal samples used in this study were anonymous and derived from a
564 biorepository of a longitudinal study approved by the ethics committee of Universidad Peruana de
565 Cayetano Heredia (UPCH, SIDISI: 65178).

566 ## Authors Contribution

567 M.V-R., R.A., M.P., and P.M. conceived the project. M.V-R., R.A., and P.M. designed experiments.
568 M.V-R., R.A., and S.A. performed experiments. M.V-R., R.A., and P.M. analyzed the data. M.V-R.,
569 R.A., K.P., and P.M. elaborated figures and tables. R.S. and D.P. helped with data interpretation. M.V-R.,
570 R.A., S.A., K.P., and P.M. wrote the manuscript with the input of D.P., R.S., and M.P.

571 ## Disclosure of interest

572 The authors report there are no competing interests to declare.

573 ## Funding

574 This work was supported by the PROCIENCIA program of CONCYTEC (Consejo Nacional de Ciencia,
575 Tecnología e Innovación Tecnológica) with grant agreement PE501079419-2022 to PM. Seed funding
576 was provided by the Universidad Peruana de Ciencias Aplicadas (C-004-2021-2) to RA.
577 This work has received funding from the European Union's Horizon 2020 research and innovation
578 program under the Marie Sklodowska-Curie grant agreement No 872869, supporting the international
579 mobility of RA, SA, KP, PM, and RS. Additionally, this work received funding from the Fogarty
580 International Center, National Institutes of Health (D43TW001140), to MP.
581

582 ## Acknowledgments

583 We are very thankful to Dr. Maya Nadimpalli for promptly providing sequencing data of the *E. coli*
584 isolate collection used in this study.
585